Use of Classical Adsorption Theory to Understand the Dynamic Filtration of Volatile Toxicants in Cigarette Smoke by Active Carbons

Peter J. Branton[1*], Kevin G. McAdam[1], Martin G. Duke[1], Chuan Liu[1], Maria Curle[1], Michele Mola[1], Christopher J. Proctor[1] and Robert H. Bradley[2] *(1) Group Research and Development, British American Tobacco, Regents Park Road, Millbrook, Southampton SO15 8TL, U.K. (2) MatSIRC Ltd., Carbon Technology, Penrith, Cumbria CA10 1NW, U.K.*

(Received 25 November 2010; accepted 16 February 2011)

ABSTRACT: The ability of two very different active carbons, a polymer-derived carbon (with ultramicropores and supermicropores, and a large volume of "transport" pores) and a coconut shell-derived carbon (predominantly ultramicroporous), to reduce the levels of volatile toxicants in cigarette smoke has been measured and compared. The polymer-derived carbon was found to be approximately twice as effective in removing the majority of measured smoke vapour-phase toxicants compared to the coconut shell-derived carbon in three different cigarette formats and with two different smoking regimes. Single-component dynamic breakthrough experiments were conducted with benzene, acrylonitrile and 2-butanone at 298 K for beds of each carbon under dry (0% RH) and wet (60% RH) conditions. Longer breakthrough times were found with the polymer-derived carbon, and breakthrough times recorded under wet conditions were found to be up to 20% shorter than those obtained under dry conditions. Correlations between micropore volume, dynamic adsorption volume and filter bed breakthrough time have been demonstrated.

1. INTRODUCTION

Active carbons (ACs) are effective adsorbents for many volatile toxic compounds encountered in domestic and industrial situations, and they are used in a wide range of separation and recovery processes. In the present work, their performance as cigarette filter additives has been investigated with respect to the adsorption of the toxic volatile constituents of tobacco smoke (toxicants) (Fowles and Dybing 2003; Rodgman and Green 2003).

The use of active carbon in a cigarette filter for vapour adsorption is not new (Tokida *et al.* 1985; Norman 1999). The subject continues to attract research interest ranging from material characterization (Sasaki *et al.* 2008; Branton *et al.* 2009), their effectiveness in reducing volatile toxicants (Laugesen and Fowles 2005, 2006; Rees *et al.* 2007; Polzin *et al.* 2008; Hearn *et al.* 2010) and potential biological effects (Bombick *et al.* 1997; Coggins and Gaworski 2008; Gaworski *et al.* 2009).

The challenges encountered in this use are considerable, requiring the reduction in concentration of a broad range of organic and inorganic species (such as carbonyls, aromatic and unsaturated hydrocarbons, and nitrogenous species) which are present at nanogram to milligram

*Author to whom all correspondence should be addressed. E-mail: peter_branton@bat.com.

levels per cigarette in a humid smoke stream. Since the mass of active carbon which can be incorporated into a typical cigarette filter is small (of the order of tens of milligrams) and the contact time with the smoke stream is low (of the order of milliseconds), then very specific properties are required of the active carbon if effective toxicant removal is to be achieved. These requirements can be summarized as rapid adsorption kinetics, non-specific toxicant adsorption and efficacy in a humid environment.

In general, the adsorption of organic vapours by active carbon is relatively easily satisfied, since most active carbons have a significant volume of micropores (mean width < 2 nm) which adsorb vapour species of the type mentioned quite readily due to the enhanced adsorption potentials which occur in such pores (Stoeckli 1974; Everett and Powl 1976). However, the diffusion rates within micropores can be slow and for many dynamic applications it is necessary to have additional wider (transport) pores to achieve realistic adsorption volumes within the given contact time.

Virtually all active carbons have relatively hydrophilic surfaces due to the presence of chemisorbed oxygen complexes (Boehm 2002) which have a marked effect on water adsorption (Barton *et al*. 1973; Stoeckli *et al*. 1983; Bradley and Rand 1993a,b, 1995; Bradley *et al.* 2002; Andreu *et al*. 2007). Under humid conditions, the adsorption of organic species is hindered by the competitive — and rapid — adsorption of water at these sites within the active carbon structure (Dubinin and Serpinsky 1981). This fills; or blocks access to pores which are then unavailable to adsorb target species (Adams *et al.* 1988). Hence, the hydrophilic character of active carbons is recognized as a major obstacle to their use in many applications.

When selecting carbons for a specific application, two main factors need to be considered: (i) their pore characteristics, i.e. their pore-size distribution and volume, and (ii) the chemistry of the carbon surface. For use in a cigarette filter, active carbons should ideally have sufficient microporosity to allow adsorption of the volume of volatiles produced during smoking, plus a level of wider (> 2 nm) transport pores to allow dynamic adsorption at rates which give effective toxicant reduction at the attendant flow rates. A relatively hydrophobic surface is also desirable. This combination of characteristics is challenging for any single material to achieve; carbon selection and performance optimization are thus important. Carbon-screening methods for cigarette filter applications have previously been described (Mola *et al*. 2008; Branton *et al.* 2009), but as yet there are no detailed models which allow an understanding or prediction of carbon activity under the conditions encountered during the smoking process. As far as the authors are aware, there have been very few, if any, published fundamental studies of the effects of carbon surface chemistry and hydrophilicity on the deleterious effects of humidity on toxicant adsorption.

In the current study, we have examined the adsorption of a range of vapours present in cigarette smoke by two carbon adsorbents with very different pore characteristics; one coconut shell-derived and the other polymer-derived. We have attempted to relate their adsorption performance in cigarette filters to their fundamental physical characteristics and to understand these relationships within the coherent framework of adsorption science. We describe below the effects of pore volume and size distribution, derived using the Dubinin adsorption theory (Dubinin and Radushkevich 1947) and its extensions (Stoeckli 1997), to kinetic parameters obtained from an analysis of equilibrium adsorption data (Reid and Thomas 2001) and dynamic breakthrough measurements. We show that, although the presence of pores of diameter > 2 nm has an effect on dynamic adsorption, breakthrough times and volumes are clearly related to parameters derived from static equilibrium data. In particular, the micropore volume appears to be a key parameter in this respect.

2. THEORY OF VAPOUR ADSORPTION

Adsorption in micropores occurs by volume-filling, as described by the Dubinin–Radushkevich (DR) equation (Dubinin and Radushkevich 1947) which, along with some of its more recent developments (Stoeckli 1997), allows a broad appreciation of the adsorption process for specific carbon/vapour systems. It is used here to derive micropore volumes and adsorption energies from static equilibrium isotherm data for a small range of volatile organic toxicants which are commonly found in respiratory and cigarette smoke challenges. In its most general form, the equation is written:

$$W = W_0 \exp\left[-\left(A/\beta E_0\right)^2\right] \quad (1)$$

where W_0 is the characteristic micropore volume of the carbon, W is the equilibrium adsorption volume uptake at an adsorption potential $A = RT \ln(p^s/p)$ (kJ/mol), p and p^s being the equilibrium and the saturated vapour pressures of the adsorptive, respectively, R is the ideal gas constant and T is the absolute value of the adsorption temperature. The quantity A is equal to $-\Delta G$ (the differential free energy of adsorption), β describes the adsorptivity of the vapour, being normally derived by comparing its physicochemical properties to those of a suitable reference compound (traditionally benzene, such that for a vapour i, $\beta_i = V_{mi}/V_{mC_6H_6}$, where V_{mi} is the molar volume or some other physicochemical parameter of the vapour i and $V_{mC_6H_6}$ is the value for the reference, i.e. benzene) and E_0 (kJ/mol) is the characteristic adsorption energy within the micropores, being inversely related to their mean width [see equation (2) below]. The standard thermodynamic state and density of the adsorbed phase (the adsorbate) is taken to be that of the bulk liquid (Dubinin and Timofeyev 1946). In practical terms, the parameters W_0 and E_0, together with the total pore volume (V_t), provide a basis for comparing the adsorption properties of ACs. The difference between W_0 and V_t (the latter obtained near to saturation pressure) allows the calculation of the volume of wider pores (> 2 nm) present in the material. Deviations from equation (1) are sometimes observed (Marsh and Rand 1970); these may be overcome by replacing the square term in equation (1) with an exponent n which describes the micropore-size distribution, thereby leading to the more general Dubinin–Astakhov equation (Dubinin and Astakhov 1971).

In the development of Dubinin's theory, early experiments using different sized molecular probes suggested that the structural constant in the original Dubinin–Radushkevich equation, effectively E_0 of equation (1), was related to the size of the micropores. Although studies using small-angle X-ray scattering methods showed E_0 to be an inverse function of the gyration radius of the micropores (Stoeckli 1997), various subsequent studies [see, for example, Dubinin and Plavnik (1968)] have shown an empirical correlation between the micropore width (L, nm) and E_0:

$$L\,(\text{nm}) = \frac{10.8}{\left(E_0 - 11.4\right)} \quad (2)$$

This is now accepted to apply to equilibrium adsorption within the average micropore width range ($0.4 \text{ nm} < L < 2 \text{ nm}$).

In certain instances, adsorption may be influenced by a second factor — the rate of adsorption under the operating flow conditions. Dynamic adsorption models essentially reflect the mechanisms of diffusion in porous carbons; they are invariably based on non-specific adsorbate–adsorbent interactions. In active carbons, there are two major barriers to diffusion: pore

entry and diffusion along the pore (Rao *et al.* 1985), the rate-limiting step in highly microporous carbons being pore entry. A number of dynamic models based on Fickian, barrier resistance/Fickian and linear driving force (LDF) models [see, for example, Reid and Thomas (2001); Rutherford and Coons (2004)] have been used to describe adsorption by granular active carbons. For microporous carbons, where pore entry is rate-determining, the kinetics are reported to follow the LDF model which treats adsorption as the mass transfer of free vapour (adsorptive) to the adsorbed phase, thereby allowing time-resolved weight change data to be fitted to a first-order rate expression and hence allowing an adsorption rate constant to be obtained (Reid and Thomas 2001). The latter method is very helpful in comparing the rates of adsorption at different adsorption pressures and different levels of pore filling.

3. EXPERIMENTAL

The two different carbon materials examined in the current study were produced using very different manufacturing processes, as shown in Figure 1 overall. The coconut shell-derived carbon used in the present work is the type of carbon currently used in many charcoal-filtered commercial cigarettes. Generic production of coconut shell-derived AC can be described as follows. The raw coconut shell material is first charred at 300–500 °C and then activated in a rotary kiln at 900–950 °C using steam, as shown in Figure 1(a). The resulting carbon is cooled, ground and sieved, resulting in irregularly-shaped carbon granules of a specified size range. The spherical particle-shaped polymer-derived carbon was prepared by a propriety process (Von Blücher and De Ruiter 2004; Von Blücher *et al.* 2006; Böhringer and Fichtner 2008), as depicted in Figure 1(b). In practice, this polymer-derived active carbon is produced via a batch process employing indirectly heated rotary kilns under reduced pressure in an inert atmosphere. After preparation of the spherical polymer feed-stock, the material is thermally stabilized using an excess of oleum. Subsequently, the material is slowly heated to 500 °C, resulting in the release of predominantly SO_2 and H_2O accompanied by carbonization of the polymer. The resulting carbon has an initial pore system which is not accessible to typical adsorptives. To create a porous system available for adsorption, the material is further heated to 900–1000 °C for activation with oxidizing agents (steam). This establishes a pore system consisting mainly of micropores with pore sizes between 0.7 nm and 3 nm. Subsequent activation with CO_2 leads to the formation of predominantly larger mesopores in the range of 3 nm to 80 nm. Combining the steam and CO_2 activation steps offers a flexible strategy for producing desired pore characteristics.

Characterization of the basic material was undertaken as follows. The general particle shape was assessed by visual inspection. The particle-size distribution was established using a sieving technique according to ASTM D2862-97 (“Standard Test Method for Particle Size Distribution of Granular Activated Carbon”). The apparent density was determined according to ASTM D2854 (“Standard Test Method for Apparent Density of Activated Carbon”), by measuring the volume of material packed by free fall from a vibrating feeder into a graduated cylinder and determining the mass of the known volume. The ash content was measured according to ASTM D2866-94 (“Standard Test Method for Total Ash Content of Activated Carbon”), in which the material was heated in a muffle furnace at 650 °C to constant weight. The weight of the resulting ashed carbon was expressed as a percentage of the weight of the original carbon sample.

Evaluation of active carbon in a cigarette filter has been described in detail elsewhere (Mola *et al.* 2008; Branton *et al.* 2009). In the current study, three different cigarette constructions were

(a) Coconut shell-derived carbon production process

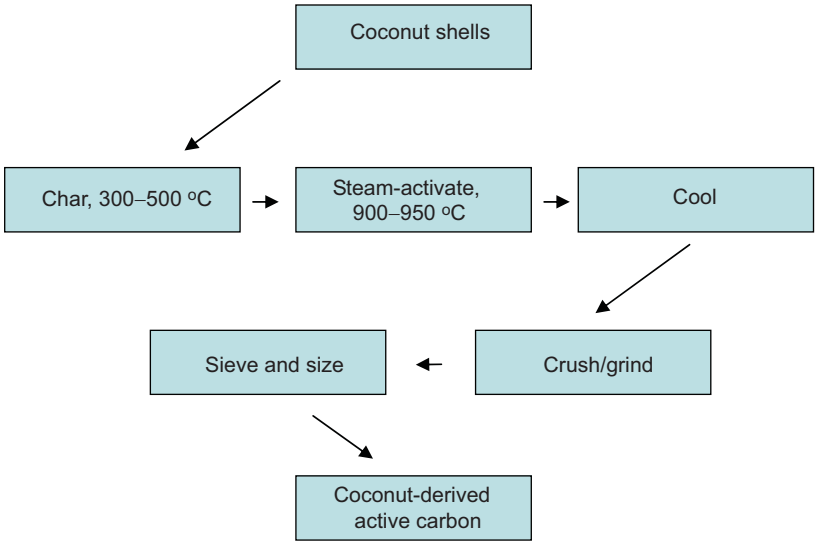

(b) Polymer-derived carbon production process

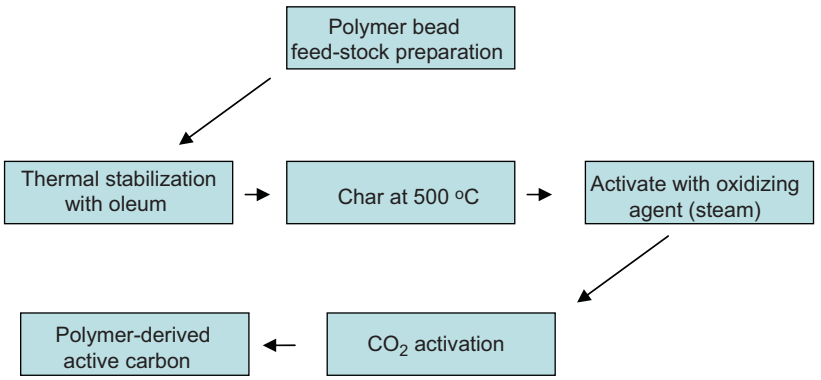

Figure 1. Production processes employed for the carbons examined in the present study.

used to test the performance of the two active carbons. Assessment of the performance of the carbons under different smoking regimes (a set of puffing parameters such as puff volume, duration and frequency of the puff) was achieved using a 24.6-mm circumference cigarette, made up of a 56 mm tobacco rod containing a Virginia-style tobacco blend (tobacco rod density = 255 mg/cm^3; moisture content = 13%) and a 27-mm length three-part cavity filter (10 mm cellulose acetate at the rod end, 4 mm cavity and 13 mm cellulose acetate at the mouth end) containing 60 ± 1 mg of each granular carbon in the filter cavity. Triacetin is used as a plasticizer on cellulose acetate filter sections and loadings of 10% and 6% by weight respectively for the mouth-end and

rod-end segments were employed. The cigarette filters were all unventilated (i.e. no air ventilation holes were made to allow influx of air during puffing). A standard 50 CU[1] permeability cigarette paper was used throughout. As a control, cigarettes of the same dimensions and composition were also prepared with an empty 4 mm filter cavity section. All cigarettes were smoked following conditioning at 22 °C and 60% RH for a period of three weeks following the inclusion of AC in the cigarette filter.

The influence of the cigarette format on the performance of the active carbon was investigated using a second, smaller circumference cigarette design. Cigarette construction in this case was a 16.9-mm circumference cigarette composed of a 56-mm long tobacco rod containing a Virginia-style tobacco blend (tobacco rod density = 240 mg/cm^3; moisture content = 13%) and a 27-mm length three-part cavity filter rod design (10 mm cellulose acetate at the rod end, 4 mm cavity and 13 mm cellulose acetate at the mouth end). The level of triacetin used on the cellulose acetate rods was 10% and 6%, respectively, by weight for the mouth-end and rod-end segments. Again, the cigarette filters were all unventilated. Due to the decreased filter volume available in the smaller circumference cigarette, 60 mg of active carbon would not fit into the filter cavity, and so 20 ± 1 mg of AC was used per filter tip. Cigarettes of the same dimensions and composition, but with an empty 4 mm filter cavity, were used as a control.

The consistency of the adsorption efficiencies of the active carbons over time in a cigarette filter was evaluated using a third cigarette format. In this case, the construction was a 24.6-mm circumference cigarette made up of a 56-mm long tobacco rod containing a US blended tobacco (tobacco rod density = 235 mg/cm^3; moisture content = 13.5%) and a 27-mm length two-part filter (15 mm cellulose acetate section at the filter mouth end and a 12 mm cellulose acetate section containing 55 ± 4 mg of interspersed activated carbon at the rod end of the filter; both cellulose acetate segments contained 7% triacetin by weight). In this study, a different approach was undertaken to incorporate the carbons into the cigarette filter to that described above; in this case, the carbon particles were interspersed amongst the cellulose acetate fibres of the filter in a commonly used commercial configuration known as a "Dual Dalmatian" design. Filter tip ventilation was added (56% at a distance of 13 mm from the mouth end) to give an ISO (ISO 3308, 2000) tar yield of ca. 7 mg. The cigarettes were packed and stored at 22 °C and 60% RH until they were smoked at time intervals of 3, 8 and 12 weeks following cigarette manufacture. As a greater number of cigarettes were available for this study, a larger number of replicate measurements were taken, allowing a statistical analysis of the data to be conducted. In the current work, MINITAB v16 was used to perform a comparison test using a General Linear Model and Tukey's method.

Smoke toxicant yields were measured (mean values of three replicates of five cigarettes for the first two studies, and mean values of five replicates of five cigarettes for the third study) using the standard ISO smoking regime (ISO 3308, 2000). This is a (bell-shaped) puff volume of 35 cm^3, puff duration of 2 s and puff interval of 1 min, with any filter-tip ventilation holes unblocked. A similar procedure was used to evaluate the carbon efficiency at a higher flow rate, using a smoking regime often referred to as the Health Canada Intense (HCI) regime (www.hc-sc.gc.ca), i.e. using a (bell-shaped) puff volume of 55 cm^3, a puff duration of 2 s and a puff interval of 30 s, with any filter-tip ventilation holes blocked. The different smoking regimes are referred to herein as ISO and HCI, respectively. Analytical methods used to quantify the selected smoke toxicants can be found at www.bat-science.com. In each case, percentage removals were calculated relative to control cigarettes containing no carbon in the filter.

[1]1 CU is the flow of air (cm^3/min) passing through a 1 cm^2 surface of the test piece at a measuring pressure of 1.00 kPa (CORESTA 1994).

Static adsorption isotherms were measured gravimetrically as described in detail elsewhere (Branton and Bradley 2009, 2011). The major interest in the present work was the dynamic adsorption of volatile toxicants; hence, for this study, 2-butanone, benzene and acrylonitrile were selected as species representative of the classes of chemical compounds adsorbed by carbon in a cigarette filter. However, since nitrogen adsorption at 77 K is firmly established for the characterization of porous solids, data for this vapour are included for completeness. The physical characteristics of the probe vapours are presented in Table 1.

TABLE 1. Adsorbate Characteristics[a]

Vapour	p^s (mbar)	V_m (cm^3/mol)	Molecular area ($\times 10^{-20}$ m^2)	Liquid density (g/cm^3)	β
Nitrogen (77 K)	989.4	17.3	16.2	0.808	0.39
Acrylonitrile (298 K)	144.7	65.5	24.94	0.806	0.74
Benzene (298 K)	126.6	88.9	30.52	0.874	1.00
2-Butanone (298 K)	127.3	89.6	30.69	0.805	1.01

[a] p^s = saturated vapour pressure; V_m = molar volume; β = affinity coefficient of equation (1) based on V_m data.

To measure the dynamic breakthrough times, a stainless-steel flow system incorporating carrier flow gas, toxicant feed, RH control, active carbon bed and bed-effluent analysis was used to compare different types of active carbons, using single challenges of the smoke toxicants listed in Table 1. Dry gaseous nitrogen at 298 K was used as the carrier, and benzene, acrylonitrile and 2-butanone were used as the individual (single) toxicant challenges. These were introduced as liquids using a motorized syringe system, evaporated and bled into the nitrogen carrier at a rate of 0.20 cm^3/min using a 20 cm^3/min nitrogen sweep from the evaporator into the main nitrogen flow of 2 ℓ/min. Using the liquid density data given in Table 1, the concentrations of toxicants at a 2 ℓ/min flow rate were 87.9 mg/ℓ, 81.0 mg/ℓ and 80.0 mg/ℓ for benzene, acrylonitrile and 2-butanone, respectively. At the higher flow rate of 5 ℓ/min, 0.66 cm^3/min of benzene or acrylonitrile was used, giving concentrations of 117.2 mg/ℓ and 108.0 mg/ℓ, respectively. Volumes are expressed as equivalent liquid volumes, as is consistent with Dubinin theory.

The carbon bed consisted of a 42-mm length of 12.6 mm o.d. (9.4 mm i.d.) stainless-steel tube which could be modified to hold different volumes of carbon using a spring-retained sliding mesh

TABLE 2. Manufacturer-supplied Carbon Characteristics

Characteristic	Activated carbon type	
	Coconut shell-derived	Polymer-derived
Particle shape	Irregular	Spherical
Particle-size distribution	0.2–0.6 mm	0.25–0.45 mm
Apparent density	0.46 g/cm^3	0.37 g/cm^3
Ash content	< 4%	0.24%

screen. For flows of 2 ℓ/min, the bed was packed to a constant volume (of ca. 6–7 cm^3) with either 3.2 g of coconut shell-derived carbon or 2.3 g of polymer-derived carbon. This gave a bed depth of ca. 90–100 mm. Beds were packed by pouring in the carbon with gentle tapping; beds packed in this manner appeared to perform effectively and no additional vibrating or tamping, etc. was used. Bed volumes of less than 6 cm^3 gave channelling effects with this experimental configuration, and thus could not be used. A Rosemount 400A HC analyzer fitted with a flame ionization detector was used to detect breakthrough. A minimum of four breakthrough tests was carried out for each system, the variation in the results being within 10%.

A "continuous" flow of 2 ℓ/min was used in the majority of the work presented here. A higher flow of 5 ℓ/min was also investigated but using 10 g of carbon in the filter, thereby giving bed volumes of ca. 20–24 cm^3. Flows were normalized to cm^3/min per g carbon to allow comparison of the results under different conditions and different carbon loadings. Carrier flows of ca. 500–700 cm^3/min per g carbon could be achieved experimentally. It is recognized that this continuous flow rate is considerably less than the peak "pulsed" flow achieved during cigarette smoking (by an order of magnitude). However, the challenge quantities of toxicant for the breakthrough test and the cigarette smoking test "*per minute*" were of a similar order of magnitude.

To study the effects of relative humidity (RH) on the breakthrough behaviour, a carrier flow containing a higher moisture content (60% RH) was used, this being produced by flowing part of the nitrogen stream (generated using a flow-splitter) through a water bubbler and then recombining it with the main flow to give the desired % RH. Again, carrier flows of 2 ℓ/min and 5 ℓ/min were used in this part of the study.

4. RESULTS AND DISCUSSION

4.1. Carbon characteristics

The basic material characteristics of the two carbons are listed in Table 2 above. The coconut shell-derived carbon possessed an irregular shape and had a reasonably wide particle-size distribution, reflecting the variable nature of the starting material and the grinding process, coupled with the size separation of the sieving process. In contrast, the polymer-derived carbon, being a synthetic material, possessed a much more closely defined spherical shape, together with a more uniform particle size. The polymer-derived material possessed a lower density, and had a lower ash content, again reflecting the synthetic nature of the polymer feedstock in comparison to the natural coconut shell-derived sample as starting materials for the carbonization processes.

4.2. Smoke toxicant yields

As described above, three series of cigarettes were used to compare the performance of the two active carbons. The first series examined the relative performances of the carbons at 60-mg loading in cavity filters of regular-sized (24.6-mm circumference) cigarettes. Two smoking regimes were used: ISO and HCI (a more intense regime with a higher linear flow rate through the filter). Smoke yields from these cigarettes are presented in Table 3. These smoke components are among those often analyzed in cigarette smoke (Baker 1999; Laugesen and Fowles 2005, 2006). The second cigarette series examined the performance of the two carbons at 20-mg loading in filter cavities of smaller circumference cigarettes. The ISO smoking regime was again used

TABLE 3. Mainstream Smoke Data Using 60 mg of Active Carbon Derived from Coconut Shell or Polymer in the Filter of a 24.6-mm Circumference Cigarette

Property	Control	Coconut-derived			Polymer-derived			Control	Coconut-derived			Polymer-derived		
	Yield per cigarette	Yield per cigarette	Amount removed	Percentage removed	Yield per cigarette	Amount removed	Percentage removed	Yield per cigarette	Yield per cigarette	Amount removed	Percentage removed	Yield per cigarette	Amount removed	Percentage removed
Smoking regime	ISO	ISO			ISO			HCl	HCI			HCI		
Puff No.	7.1	6.8			7.1			9.1	9.9			9.8		
NFDPM[a] (mg)	11.8	10.3			10			25.6	24.3			24.1		
Nicotine (mg)	0.94	0.85			0.83			2.02	1.99			1.87		
Water (mg)	3.1	2.3			1.7			16.3	16.1			15.7		
CO (mg)	11.4	11.5			11.5			21.4	21.6			22.8		
Acetaldehyde (µg)	584	384	200	34	289	295	51	1030	863	167	16	860	170	17
Acetone (µg)	281	155	126	45	40	241	86	499	358	141	28	204	295	59
Acrolein (µg)	78.4	39	39.4	50	11.9	66.5	85	144.2	93.7	50.5	35	53.7	90.5	63
Butyraldehyde (µg)	38.9	20.5	18.4	47	4.5	34.4	88	77.1	51.3	25.8	33	19.2	57.9	75
Crotonaldehyde (µg)	23.9	10.2	13.7	57	2.2	21.7	91	49.4	26.5	22.9	46	6.5	42.9	87
Formaldehyde (µg)	59.3	35.5	23.8	40	27	32.3	54	119.1	68.7	50.4	42	52.3	66.8	56
2-Butanone (µg)	69.7	34.5	35.2	51	4.5	65.2	94	132.2	85.1	47.1	36	26.4	105.8	80
Propionaldehyde (µg)	49.4	27.3	22.1	45	8.2	41.2	83	86.7	61.9	24.8	29	43.1	43.6	50
HCN (µg)	118.6	66.1	52.5	44	54.9	63.7	54	260.6	195.9	64.7	25	180.1	80.5	31
1,3-Butadiene (µg)	20.0	16.0	4.0	20	3.4	16.6	83	53.7	41.7	12	22	22.8	30.9	58
Acrylonitrile (µg)	8.7	4.8	3.9	45	1.4	7.3	84	18.8	12.9	5.9	31	6	12.8	68
Benzene (µg)	32	18.2	13.8	43	5.1	26.9	84	59.8	42.6	17.2	29	12.1	47.7	80
Isoprene (µg)	199	117	82	41	21	178	89	420	324	96	23	76	344	82
Toluene (µg)	45.7	29.5	16.2	35	18.1	27.6	60	100.2	74.0	26.2	26	37.8	62.4	62

[a]NFDPM = Nicotine Free Dry Particular Matter (tar).

with these cigarettes; however, due to the smaller volume of the reduced circumference filter, the flow rate through the carbon beds was higher, and hence the residence time was shorter than with regular-sized cigarettes smoked under the ISO regime. The smoke yields from these cigarettes are presented in Table 4. The third series of cigarettes examined the relative performance of the carbons dispersed amongst the cellulose acetate fibres of a regular circumference cigarette under the ISO smoking regime. Measurements were taken at three time intervals, viz. 3, 8 and 12 weeks after manufacture of the cigarettes, as listed in Table 5.

The data presented in Tables 3–5 show that the three series of cigarettes generated different quantities of tar [Nicotine Free Dry Particulate Matter (NFDPM)]; the first series generated 10–12 mg of tar under the ISO regime and 24–25 mg under the HCI regime. The second series generated 8–9 mg of tar and the third series generated 6–7 mg of tar, both under the ISO smoking regime. There were also differences in the tobacco blends between the three series of cigarettes, which may have further resulted in differences in the yields of individual smoke constituents from the different series of cigarettes (Gregg *et al*. 2003). However, the blend type would not have affected the performance of the carbon. The combination of these two factors means that it is difficult to directly compare the smoke yields of individual smoke constituents amongst cigarettes from different series. The data in Tables 3 and 4 also show that there were slightly lower tar yields (10–20%) from cigarettes containing carbon filters than from the respective cellulose acetate filter control cigarettes.

TABLE 4. Mainstream Smoke Data Using 20 mg of Active Carbon Derived from Coconut Shell or Polymer in the Filter of a 16.9-mm Circumference Cigarette

Property	Control	Coconut shell-derived			Polymer-derived		
	Yield	Yield	Amount removed	Percentage removed	Yield	Amount removed	Percentage removed
Puff No.	6.1	5.9			6.1		
NFDPM[a] (mg)	8.9	7.9			8.0		
Nicotine (mg)	0.82	0.74			0.78		
Water (mg)	3.7	2.4			2.7		
CO (mg)	6.4	5.9			6.3		
Acetaldehyde (µg)	286	235	51	18	215	71	25
Acetone (µg)	145	109	36	25	75	70	48
Acrolein (µg)	38.7	27.9	10.8	28	19.3	19.4	50
Butyraldehyde (µg)	21.0	15.3	5.7	27	8.9	12.1	58
Crotonaldehyde (µg)	11.8	7.7	4.1	34	3.6	8.2	69
Formaldehyde (µg)	46.0	34.6	11.4	25	30.6	15.4	33
2-Butanone (µg)	37.1	26.4	10.7	29	14.5	22.6	61
Propionaldehyde (µg)	25.6	19.7	5.9	23	14.2	11.4	45
HCN (µg)	76.3	59.1	17.2	23	62.9	13.4	18
1,3-Butadiene (µg)	12.7	14.1	–1.4	–11	10.1	2.6	20
Acrylonitrile (µg)	8.0	7.1	0.9	11	4.8	3.2	40
Benzene (µg)	24.2	21.9	2.3	10	10.7	13.5	56
Isoprene (µg)	236	229	7	3	133	103	44
Toluene (µg)	34.6	31.1	3.5	10	11.5	23.1	67

[a]NFDPM = Nicotine Free Dry Particulate Matter (tar)

TABLE 5. Effect of Ageing Time on Smoke Yields for Cigarettes with Filters Containing Coconut Shell- and Polymer-derived Active Carbons

Property	Coconut shell-derived carbon aged for						Polymer-derived carbon aged for					
	3 weeks		8 weeks		12 weeks		3 weeks		8 weeks		12 weeks	
	Yield	SD	Yield	SD	Yield	SD	Yield	SD	Yield	SD	Yield	SD
Puff No.	7.5	0.1	7.8	0.3	7.6	0.2	7.5	0.4	7.5	0.2	7.8	0.3
NFDPM[a] (mg)	6.4	0.29	7.0	0.59	6.2	0.37	6.8	0.23	6.3	0.23	6.3	0.11
Nicotine (mg)	0.55	0.03	0.59	0.05	0.57	0.02	0.55	0.01	0.55	0.03	0.53	0.02
Water (mg)	0.58	0.07	0.8	0.13	0.6	0.09	0.6	0.07	0.5	0.04	0.6	0.10
CO (mg)	6.3	0.31	6.4	0.40	6.3	0.23	6.3	0.21	5.5	0.35	5.4	0.14
Acetaldehyde (µg)	171	23.3	204	15.1	190	26.7	100	17.1	116	33.1	118	9.09
Acetone (µg)	73.3	9.38	80.0	9.17	72.6	11.5	20.4	5.28	24.5	8.14	28.0	3.23
Acrolein (µg)	12.8	1.77	13.6	2.10	14.9	3.14	3.9	0.91	4.4	1.67	5.8	0.44
Butyraldehyde (µg)	10.0	1.11	10.2	0.99	8.76	1.23	3.0	0.58	3.2	0.89	3.5	0.38
Crotonaldehyde (µg)	2.81	0.71	2.06	0.54	1.72	0.52	< LOQ[b]	–	< LOQ	–	< LOQ	–
Formaldehyde (µg)	8.25	0.88	9.20	1.23	8.8	1.25	7.4	0.86	8.8	1.18	9.6	1.07
2-Butanone (µg)	17.9	2.75	17.5	2.35	13.8	2.44	3.6	1.07	4.3	1.68	5.0	0.77
Propionaldehyde (µg)	13.9	1.57	15.2	1.42	14.0	2.14	4.8	1.00	5.3	1.61	6.7	0.55
HCN (µg)	25.1	3.77	27.2	1.27	38.2	7.63	27.7	4.50	26.6	4.93	24.5	2.55
1,3-Butadiene (µg)	14.5	2.23	10.8	1.44	12.1	3.28	5.9	1.00	4.25	0.62	< LOQ	–
Acrylonitrile (µg)	3.0	0.42	2.44	0.35	2.4	0.39	1.7	0.14	< LOQ	–	< LOQ	–
Benzene (µg)	9.8	1.60	8.84	1.58	9.6	1.19	< LOQ	–	< LOQ	–	< LOQ	–
Isoprene (µg)	38.9	13.1	40.9	8.86	51.6	13.5	< LOQ	–	< LOQ	–	< LOQ	–
Toluene (µg)	12.09	1.93	10.33	1.93	16.7	1.60	< LOQ	–	< LOQ	–	< LOQ	–

[a]NFDPM = Nicotine Free Dry Particulate Matter (tar). [b]< LOQ = below the limit of quantification (crotonaldehyde, 1.1 µg/cigarette; 1,3-butadiene, 1.38 µg/cigarette; acrylonitrile, 1.31 µg/cigarette; benzene, 1.4 2 µg/cigarette; isoprene, 8.2 µg/cigarette; toluene, 2.10 µg/cigarette).

Smoke yields for the 24.6-mm circumference cigarettes under both ISO and HCI regimes are listed in Table 3, together with the percentage reductions relative to a cigarette with an empty filter cavity. Both carbons were effective vapour adsorbents in these cigarette filters, offering substantial reductions in the yields of many of the 14 volatile smoke toxicants measured in this study. Under the ISO smoking regime, the coconut shell-derived carbon reduced most constituents by 40–60%; however, acetaldehyde, 1,3-butadiene and toluene were removed less effectively (at 20–35% efficiency). Most constituents were adsorbed more effectively by the polymer-derived carbon under the ISO regime — with reductions of the order of 80–95% being observed for smoke toxicants other than formaldehyde, acetaldehyde, hydrogen cyanide (HCN) and toluene (50–60% reductions). Under the HCI regime, the mass of smoke constituents removed by the carbon filters was higher than that found under the ISO regime; however, when expressed as a percentage of the control cigarette yields, the removal efficiency of both carbons under the HCI regime was lower than that under the ISO regime. Under HCI conditions, the coconut shell-derived carbon filtered cigarettes provided reductions of the order of 25–45% for most smoke constituents, other than acetaldehyde (16%). The polymer-derived carbon cigarettes reduced most smoke constituent yields by 60–90%, other than acetaldehyde and HCN (15–30%).

Table 4 shows the ISO smoke data from the smaller circumference cigarette series. Again, both active carbons reduced smoke yields across the range of measured smoke toxicants, with the exception of 1,3-butadiene for the coconut shell-derived carbon where yields appeared to increase slightly. The extent of the reductions relative to the non-carbon filtered control cigarettes was less than that found with the first series of cigarettes reported above. The coconut shell-derived carbon filter reduced the yields of most measured smoke constituents by 20–35%, other than acrylonitrile and the four hydrocarbon species where reductions were at ca. 10% level. The polymer-derived carbon filter resulted in more effective reductions in smoke constituent levels than the coconut shell-derived carbon, with the exception of HCN. With most of the measured smoke constituents, use of the polymer-derived carbon filter resulted in reductions of 40–70%; exceptions to this were HCN (18%), 1,3-butadiene (20%), acetaldehyde (25%) and formaldehyde (33%). The lower percentage reductions in smoke analytes were due to the lower weight of AC used in this experiment, and also the reduced contact times in the smaller filter.

Ageing, or a decline in adsorption efficiency over time, is a phenomenon that has been observed previously with carbon filters (Branton and Bradley 2010) and is a consequence of the presence of tobacco volatiles, water vapour and the triacetin plasticizer in the filter. Table 5 lists the smoke yields from both cigarette types over a time period of 3 to 12 weeks. The yields of a number of smoke constituents from one or both of these cigarettes were below the limits of quantification of the analytical methodology and could not be included in the data analysis. The data from Table 5 on the cigarettes used for the ageing study again show substantially lower yields for the majority of the volatile toxicants examined from cigarettes with polymer-derived carbon filters as opposed to coconut shell-derived carbon filters. Two exceptions were found to this trend — formaldehyde and HCN, where comparable yields were measured from the two cigarette types. Ageing was not found to be a measurable phenomenon with coconut shell-derived carbon filter cigarettes for most of the measured constituents; however, HCN and toluene yields showed a statistically significant increase over the 3 to 12 weeks period. The yields of isoprene also showed a numerical increase over this time, but the trend was not significant at the 95th percentile level. With the polymer-derived filter cigarettes, the yields of acrolein, formaldehyde and propionaldehyde showed significant increases over this time period. The yields of HCN, acetaldehyde, acetone, butyraldehyde and 2-butanone also showed numerical increases over this time period, but the increases were not significant at the 95th percentile level. It may be that the resolving power of

the experimental methods employed was insufficient to establish the statistical significance for these increases. Taken as a whole, these observations suggest a slightly greater ageing effect for the polymer-derived carbon over this time period. The extent of ageing in each case was small in comparison to the differences in toxicant removal efficiencies between the two carbons.

Thus, overall, the polymer-derived carbon was a more effective adsorbent for cigarette smoke vapour phase toxicants than the coconut shell-derived carbon currently used in carbon-filtered cigarettes. The nature of the smoke constituent being removed is very important in terms of the effectiveness of the carbon filters. Under ISO and HCI conditions, the polymer-derived carbon was approximately twice as effective as the coconut shell-derived carbon in reducing most of the measured smoke constituent yields. However, with formaldehyde and hydrogen cyanide, the performance of the two carbons was much closer. Ion-exchange resins have been investigated for the effective selective filtration of aldehydes and HCN (Branton *et al.* 2011). Historically, these constituents have been shown to have a proportion of their yields bound to the particulate phase of smoke (Baker 1999) and therefore unavailable for adsorption by carbon filters. It is also likely that with higher flow-rate conditions than those found with the ISO smoking regime and a standard circumference cigarette (i.e. a lower circumference cigarette under ISO or a standard circumference cigarette under HCI), the effectiveness of the two carbons towards acetaldehyde would be similar. The similar performance of the carbons towards acetaldehyde under high flow-rate conditions is likely to reflect the high vapour pressure and low condensability of this compound under smoking conditions, leading to the need for a residence time over the carbon that is longer than that found with high flow-rate smoking conditions. Acetaldehyde was also present at considerably higher yields than any of the other constituents examined in this work; indeed, these experiments have highlighted a limitation in the overall quantity of acetaldehyde that can be removed by carbons under flow conditions in cigarettes. In contrast, 1,3-butadiene was much more effectively removed by the polymer-derived carbon than the coconut shell-derived material, and a similar picture was observed for the other hydrocarbons under high flow-rate smoking conditions. These observations suggest a mass-transport related limitation in performance with conventional coconut shell-derived carbons for these smoke constituents.

4.3. Equilibrium adsorption characteristics

Characteristic data derived from static adsorption studies for the two carbons studied are listed in Table 6 overleaf. The adsorbed volumes which resulted from analyses of equilibrium adsorption data show that the coconut shell-derived material had a BET surface area of 690–980 m^2/g (depending upon the adsorption vapour) and possessed a homogeneous structure containing 0.40 cm^3/g micropores (< 2 nm). Further analysis showed that 60–70% of these pores had a mean width less than 1 nm. These pores are termed ultramicropores and it is within these pores that the adsorption potentials are likely to be the highest. The only other porosity in this material was a very low volume (0.02 cm^3/g) of pores with widths greater than 2 nm.

In sharp contrast, the polymer-derived carbon had a larger BET surface area of 1150–1660 m^2/g, and a greater total measured pore volume of 0.9–1.3 cm^3/g of which ca. 0.7 cm^3/g was in the micropore-size range. A high volume of the micropores were supermicropores, i.e. they possessed mean widths of 1–2 nm; however, the overall balance of the porosity resided in pores with widths greater than 2 nm. The inverse relationship [equation (2)] between the adsorption energy (E_0, kJ/mol) of the Dubinin concept and the mean micropore width (L, nm) based on the SAXS and SANS scattering properties of the graphene planes which form the micropore walls, led to micropore dimensions of 1.2–2.2 nm: the latter value is (with an error ±10%) at the

TABLE 6. Carbon Characteristic Data Derived from Static Adsorption Isotherms[a]

Adsorbate	BET area (m^2/g)	W_0 (cm^3/g)	V_t (cm^3/g)	$V_t - W_0$ (cm^3/g)	E_0 (kJ/mol)	L (nm)
Coconut shell-derived carbon						
Acrylonitrile	780	0.41	0.42	0.01	28.1	0.64
Benzene	850	0.38	0.40	0.02	31.8	0.53
2-Butanone	690	0.39	0.41	0.02	30.7	0.56
Nitrogen (at 77 K)	980	0.42	0.40	0.02	24.7	0.81
Polymer-derived carbon						
Acrylonitrile	1310	0.75	1.05	0.30	16.6	2.10
Benzene	1150	0.70	1.25	0.55	20.1	1.24
2-Butanone	1210	0.72	1.30	0.58	20.0	1.26
Nitrogen (at 77 K)	1660	0.57	0.94	0.37	16.3	2.20

[a]W_0 = micropore volume; V_t = total pore volume; E_0 = Dubinin energy; L = micropore mean width.

upper limit of the IUPAC classification of micropores. These figures confirm the greater surface area and wider microporosity of the polymer-derived carbon compared to the values for the coconut shell-derived material. The increased pore volume of the polymer-derived carbon compared to that of the coconut shell-derived carbon was a consequence of the addition of meso-/macro-pores to its structure. It has previously been shown (Branton *et al.* 2009) that the addition of meso-/macro-pores leads to a greater filtration efficiency than simply increasing the micropore volume over the range used here.

4.4. Adsorption kinetics

Table 7 overleaf presents adsorption rate constants for the two carbons and four vapours studied, as derived using a first-order mass-transport Linear Driving Force (LDF) model. The results show higher rate constants for the polymer-derived material for benzene and nitrogen, but lower rate constants with acrylonitrile and 2-butanone. Comparative analysis of the rate constants obtained across a broad range of relative pressure and pore-filling showed that, for the polymer-derived carbon, even the micropore volumes (which were high compared to those of the coconut shell-derived material) exhibited relatively rapid adsorption. Thus, a notable feature of the polymer-derived carbon was the significantly higher volume of micropores possessing a well-developed supermicroporosity. In addition, approximately half of the total volume of pores were wider than 2 nm, which is the size range often associated with improved intra-granular molecular diffusion. Indeed, these types of pores are frequently referred to as transport pores. Although the coconut shell-derived carbon had a very different structure, which was effectively homogeneous and microporous with virtually no transport pores, nevertheless these pores filled relatively rapidly for two of the vapours of interest. It is therefore concluded that the actual rates of adsorption are complex and a greater study of adsorbate–adsorbent interactions would be required before the precise behaviour can be understood.

TABLE 7. Rate Constants, k, and Corresponding Polanyi Adsorption Potentials [A = RT ln(p^s/p)] for Micropore Filling in Cigarettes with Filters Containing Coconut Shell- and Polymer-derived Active Carbons

Adsorbate	Coconut shell-derived			Polymer-derived		
	p/p^s Range	$k \times 10^{-2}$ (s^{-1})	A (kJ/mol)	p/p^s Range	$k \times 10^{-2}$ (s^{-1})	A (kJ/mol)
Acrylonitrile (298 K)	0.010–0.020	3.78	11.82	0.010–0.020	2.04	11.72
	0.020–0.030	2.43	11.31	0.020–0.030	1.89	11.30
	0.040–0.050	1.97	10.81	0.040–0.050	2.10	11.03
Benzene (298 K)	0.025–0.050	0.77	10.12	0.020–0.050	2.11	10.10
	0.049–0.099	1.08	9.72	0.050–0.101	2.40	9.42
	0.250–0.298	0.89	9.03	0.250–0.301	2.11	9.20
2-Butanone (298 K)	0.010–0.020	1.62	10.40	0.010–0.023	1.04	11.40
	0.020–0.030	1.80	8.00	0.020–0.030	0.92	7.97
	0.040–0.050	1.30	7.67	0.040–0.050	0.90	7.71
Nitrogen (77 K)	0.009–0.013	3.08	10.82	0.005–0.006	3.85	11.15
	0.025–0.034	2.76	9.84	0.026–0.036	4.75	10.09
	0.052–0.071	2.06	9.11	0.055–0.074	4.51	9.06

4.5. Dynamic breakthrough measurements

Table 8 shows the breakthrough times and volumes at a flow rate of 2 ℓ/min for benzene, acrylonitrile and 2-butanone, and at a flow rate of 5 ℓ/min for benzene and acrylonitrile. Measurements were made at 0% RH and 60% RH on both carbons. The breakthrough time, t_{bt}, was derived from the general expression:

$$t_{bt}\ (\text{min}) = \frac{\text{wt. carbon (g)} \times V_{da}\ (\text{cm}^3/\text{g})}{C_{tox.}\ (\text{cm}^3/\text{min})} \quad (3)$$

where $C_{tox.}$ is the concentration of toxicant in the influent stream — expressed as a liquid volume using density data from Table 1 — and V_{da} is the relevant adsorption volume of the carbon.

TABLE 8. Breakthrough Time (t_{bt}) and Volume (V_{bt}) for Active Carbons at 298 K and 0% RH and 60% RH

(a) Measured at a flow rate of 2 ℓ/min (3.2 g coconut shell-derived carbon or 2.3 g polymer-derived carbon beds; toxicant challenge = 0.20 cm^3/min)

	Breakthrough time, t_{bt} (min)		Breakthrough volume, V_{bt} (cm^3/g)	
	0% RH	60% RH	0% RH	60% RH
Polymer-derived carbon				
Benzene	7.2	6.7	0.63	0.59
Acrylonitrile	5.9	5.7	0.52	0.50
2-Butanone	7.0	6.8	0.61	0.60
Coconut shell-derived carbon				
Benzene	5.7	5.4	0.36	0.34
Acrylonitrile	5.4	5.2	0.34	0.32
2-Butanone	5.6	5.3	0.35	0.33

(b) Measured at a flow rate of 5 ℓ/min (10 g coconut shell-derived carbon or polymer-derived carbon beds; toxicant challenge = 0.66 cm^3/min)

	Breakthrough time, t_{bt} (min)		Breakthrough volume, V_{bt} (cm^3/g)	
	0% RH	60% RH	0% RH	60% RH
Polymer-derived carbon				
Benzene	8.7	7.1	0.57	0.47
Acrylonitrile	7.2	5.7	0.47	0.38
Coconut shell-derived carbon				
Benzene	6.3	5.3	0.42	0.35
Acrylonitrile	5.8	4.7	0.38	0.31

The data listed in Table 8 show that, under dry conditions, the toxicant breakthrough times increased with the micropore and total pore volumes of the carbon as derived from equilibrium data. This was true for both flow rates investigated. Thus, the higher pore volume of the polymer-derived carbon was very effective in extending the breakthrough time for these probe vapours (adsorbates). This is consistent with the improved dynamic adsorption predicted from the kinetic analysis of the equilibrium data.

If it is assumed that the standard state applies to dynamic adsorption and that the density of the adsorbed toxicant phase is equal to that of the bulk liquid at $T_{ads.}$ (Dubinin and Timofeyev 1946), then the corresponding volumes adsorbed at breakthrough (V_{bt}) can be calculated using:

$$V_{bt}\ (cm^3/g) = \frac{t_{bt}\ (min) \times C_{tox.}\ (cm^3/min)}{wt.\ carbon\ (g)} \quad (4)$$

Equation (4) is largely a re-arrangement of equation (3), with V_{bt} and V_{da} being notionally the same. However, as with the values of W_0, variations are likely to occur according to the adsorbate in question. Since, under non-equilibrium adsorption conditions, factors such as vapour pressure, molecular size, shape and chemistry may significantly influence the adsorption process, a distinction is made here between the two parameters.

When equation (4) was used, a clear difference between the two carbon types was evident, with the V_{bt} values from the polymer-derived carbon being significantly higher than those from the coconut shell-derived material. However, the V_{bt} value for each material correlated very closely with the corresponding micropore volume (W_0, cm^3/g) calculated from the equilibrium data. This is clearly shown in Figure 2 and is also seen from a comparison of the respective values listed in Tables 6 and 8. As expected, the values of t_{bt} listed in Table 8 vary between the two different testing regimes, each with different carrier flows and challenge concentrations. These values would also be dependent on other experimental variables, such as bed volume and configuration, etc. However,

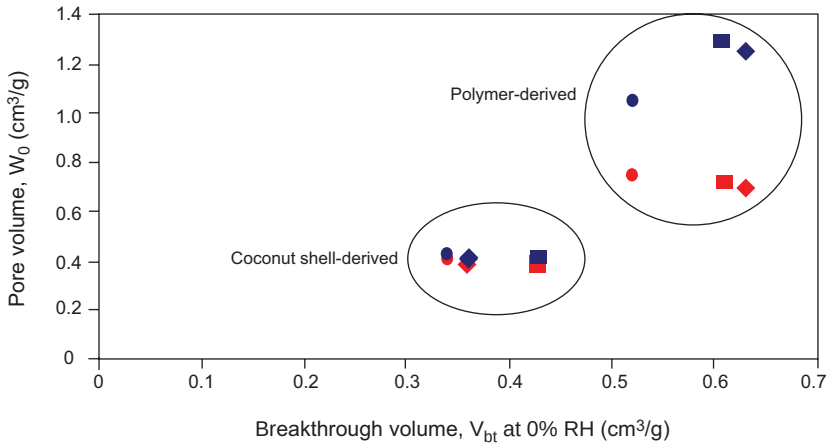

Figure 2. Relationship between the pore volumes, W_0, derived from equation (1) and the total pore volumes, V_t, obtained from static adsorption isotherm measurements with the values of V_{bt} obtained from dynamic breakthrough data measured at a flow rate of 2 ℓ/min. Note the distinct populations for each carbon. Data points correspond to the following adsorbates: ●, acrylonitrile; ◆, benzene; ■, 2-butanone. Those corresponding to micropore volume are shown in red while those for total pore volume are shown in dark blue.

the actual volume of toxicant adsorbed by each carbon is an absolute property. That this matches so closely with the micropore volume calculated from equation (1) is perhaps surprising. The similarity between V_{bt} and W_0 for the highly microporous coconut shell-derived material is intriguing. In view of the narrow porosity present in this carbon, a negative impact might have been expected on diffusion and pore-filling under dynamic conditions. It may therefore be misleading to assume that the superior performance of the polymer-derived carbon resulted merely from the improved adsorption kinetics, since the narrow microporosity of the coconut shell-derived carbon did not appear to significantly restrict micropore filling in the dynamic situations encountered in the present study. In any event, the V_{bt} data for both carbons indicate quite clearly that a high percentage of the total volume was filled under dynamic conditions, which is very encouraging in terms of achieving effective adsorption under practical conditions.

Preliminary work applying similar techniques to breakthrough data for a tertiary mixture of toxicants (acrylonitrile, benzene and 2-butanone) has indicated that breakthrough times for individual vapours (t^1_{bt} , t^2_{bt}, etc.) result from the specific interactions of the vapour with the carbon porosity (and surface chemistry) and that this results in individual breakthrough volumes whose sum, i.e. the total breakthrough volume, V_{bt}, coincides with W_0 such that:

$$V_{bt} = V_1^{\alpha_1} + V_2^{\alpha_2} + V_3^{\alpha_3} \quad (5)$$

where the superscript α_x describes the dynamic adsorbability of the vapour (x). The dynamic adsorption performance is therefore a fundamental property resulting from the structural characteristics of the carbon and it is this property which determines the breakthrough volume and hence the breakthrough time, t_{bt}.

Our work on single vapour systems under dry conditions to date has shown that the total pore volume of a carbon, and its micropore volume in particular, are critical parameters in selecting carbons for dynamic filtration purposes. The application of classical theory to equilibrium adsorption data provides a firm basis for both carbon selection and performance prediction in dynamic and extreme applications. For single vapour challenges, it appears that it is something close to micropore filling which determines breakthrough and, hence, we have assumed that the properties of the adsorbed phase are the same as those of the bulk liquid. For mixed vapour challenges, we propose that the resultant breakthrough volume should be composed of an adsorbate mixture whose composition reflects the relative adsorbability of the individual vapours in the challenge. Wider ranging tests are required to examine whether the relative adsorbabilities can be derived absolutely from the physicochemical properties of the pure vapours, i.e. from a modified value of β in equation (1) for example. Whilst the order of breakthrough for the vapours studied thus far follows that indicated by their β value, this requires further study before a firm basis of prediction is possible. As outlined above, it is generally accepted that the standard state of the adsorbed phase is that of the bulk liquid at the corresponding temperature, with possible exceptions being for the filling of the narrower micropores where packing constraints restrict the usual coordination of the molecules in the liquid. This concept has been studied for classical adsorption probes such as nitrogen at 77 K (Aukett *et al*. 1992), but only preliminary work has been carried out on organic vapour systems (Bradley and Rand 1993b, 1995). For mixed adsorbate systems, on the one hand, one might expect these packing effects to be exacerbated, leading to a density for the adsorbed phase which is less than that of the bulk liquid. On the other hand, however, cooperative effects, interstitial packing of one size of vapour molecule within the gaps between others of different size, and even solubility parameters may be relevant.

The trends in the smoke yield results also correlate well with those obtained from breakthrough measurements (using benzene, acrylonitrile and 2-butanone as probe molecules), despite the fact that conditions were quite different; e.g. continuous versus pulsed flow, the presence of many other vapour/aerosol species in smoke. Hence, measuring breakthrough profiles may be a useful predictive tool for the screening of ACs for use in cigarette filters.

The presence of water vapour can also have a significant effect on toxicant adsorption. It is known that water rapidly adsorbs at hydrophilic centres (Barton *et al*. 1973; Stoeckli *et al.* 1983; Bradley and Rand 1993a,b; Bradley *et al.* 2002), which in carbons are mainly chemisorbed oxygen functionalities present on the edges of the carbon graphene planes (Boehm 2002; Andreu *et al*. 2007). Hence, they are located near to the micropore entrances and extend into the wider carbon porosity, i.e. the heterogeneous or isotropic domains. Adsorbed water fills part of the available adsorption space and also blocks access to other regions of porosity, a factor which is known to decrease adsorption efficiency towards organic species causing a decrease in t_{bt} (Adams *et al*. 1988). This effect is clearly seen by comparing the data listed in Table 8 for dry (0% RH) and wet (60% RH) streams of 5 ℓ/min flow rate. The data clearly show reductions in breakthrough times of 16–18% being recorded for benzene on both carbons and decreases of 19–21% for acrylonitrile in higher humidity vapour streams. Similar effects, although slightly less prominent in terms of percentage reduction, may be observed for the 2 ℓ/min flow rate data.

As a means of understanding the ageing behaviours of the two carbons observed in cigarette filters, the impact of moisture on breakthrough times and volumes was compared. Very similar sensitivities were observed for the two carbons under 2 ℓ/min flow conditions. The two carbons also showed a similar sensitivity to moisture under 5 ℓ/min flow conditions, albeit with the possibility of a marginally greater impact on the polymer-derived carbon. However, such small differences are likely to lie within experimental error and cannot therefore be taken as indicating a real difference in the properties of the two carbons.

5. CONCLUSIONS

Two very different active carbons were assessed for their efficiency in adsorbing certain smoke constituents when used as filter adsorbents in cigarettes. A new polymer-derived material was found to be approximately twice as effective, in general, in removing volatile cigarette smoke toxicants than the coconut shell-derived carbon commonly used in contemporary carbon-filtered cigarette products. The polymer-derived carbon performed well at both ISO and HCI smoking regimes, and with regular and smaller circumference cigarettes. However, limitations were observed under higher flow-rate smoking conditions in the capabilities of the two carbons towards the adsorption of acetaldehyde and of the coconut shell-derived carbon towards some hydrocarbons. The performance of the coconut shell-derived carbon as a filter adsorbent was largely stable over the period of 3 to 12 weeks, whereas the performance of the polymer-derived carbon towards a wide range of constituents diminished over the same time period.

By applying adsorption first principles to equilibrium isotherm data and also measuring dynamic breakthrough times and volumes, we have established criteria by which active carbon performance towards the removal of various toxicants from challenge streams (characterized by relatively high flows per weight of carbon and short contact times) can begin to be understood. This approach identifies some of the key factors which influence dynamic toxicant adsorption and hence provides a basis for both selecting ACs for cigarette filter and other filter applications, and also for predicting carbon performance in this use.

The classical Dubinin–Radushkevich equation is an effective means of deriving characteristic information about active carbons from equilibrium adsorption data which correlates with, and allows an understanding of, their performance in dynamic separation situations. Measurements of pore volumes, followed by the calculation of intrinsic energies and dimensions, yield fundamental information concerning carbon structure and adsorption behaviour. These factors influence the way adsorption equilibrium is reached in static measurements and, in a general manner, reflected in the rate constants obtained using the first-order mass-transfer (LDF) approach. Perhaps what is surprising is that the pore volume parameters derived from equilibrium data are so closely reproduced in the dynamic situation, which makes the use of the former such a powerful tool in carbon screening and selection situations.

As a consequence, dynamic breakthrough data measured for beds of each carbon under dry conditions correlated well with static adsorption isotherm data. For each vapour studied, a longer breakthrough time (t_{bt}) correlated with higher W_0 values. We believe that a similar behaviour occurs for mixed vapour challenges, although preliminary data appear to indicate that the adsorbed phase is likely to obey the law of mixtures, with its composition reflecting relative concentration in the influent stream modified by its dynamic adsorbability on the carbon in question. In all our work to date, the value of W_0 has been found to correlate so closely with V_{bt} that it seems only reasonable to use it as a basis for the further development of predictive methods in this field. One very clear challenge for the future is the identification of the physicochemical factors which govern the order of breakthrough for specific vapour mixtures, plus the effect(s) on this of carbon porosity and surface chemistry. The use of β, or a modified form of β, may be useful in this respect.

Breakthrough times measured under wet conditions were always shorter than those obtained under dry conditions and the V_{bt} values show that, under these circumstances, a commensurate volume of the porosity was not used due to competitive water vapour adsorption which blocked certain areas of porosity. The overall effect of humidity in the influent stream was a reduction in carbon capacity and efficiency as reflected in a shorter breakthrough time.

It is rewarding that the application of a basic and theoretical approach provides a greater understanding of key factors relevant to this specific application. The greatest reductions in toxicant in levels cigarette smoke were achieved when the breakthrough times in the dynamic tests were the longest.

Although this present work has been focused on the adsorption of volatile smoke toxicants, the underlying principles of carbon characteristic properties and behaviour can be extended to many other complex separation applications. Cigarette smoke also contains other toxicants that predominantly exist in aerosol droplets (Baker 1999). These species will not be available for adsorption and their reduction has to be achieved by other means (McAdam *et al*. 2011; Liu *et al*. 2011).

ACKNOWLEDGEMENT

The spherical activated carbon was supplied by Blücher GmbH.

REFERENCES

Adams, L.B., Hall, C.R., Holmes, R.J. and Newton, R.A. (1988) *Carbon* **26,** 451.
Andreu, A., Stoeckli, H.F. and Bradley, R.H. (2007) *Carbon* **45,** 1854.
Aukett, P.N., Quirke, N., Riddiford, S. and Tennison, S.R. (1992) *Carbon* **30,** 913.

Baker, R.R. (1999) in *Tobacco, Production Chemistry and Technology*, Davis, D.L., Nielsen, M.T., Eds, Blackwell Science, Malden, MA, U.S.A., pp. 398–439.
Barton, S.S., Evans, M.J.B. and Harrison, B.H. (1973) *J. Colloid Interface Sci.* **45,** 542.
Boehm, H.P. (2002) *Carbon* **40,** 145.
Böhringer, B. and Fichtner, S. (2008) *Pat. No. WO002008110233*.
Bombick, D.W., Bombick, B.R., Ayres, P.H., Putnam, K., Avalos, J., Borgerding, M.F. and Doolittle, D.J. (1997) *Fundam. Appl. Toxicol.* **39,** 11.
Bradley, R.H. and Rand, B. (1993a) *Carbon* **31,** 269.
Bradley, R.H. and Rand, B. (1993b) *Fuel* **72,** 389.
Bradley, R H. and Rand, B. (1995) *J. Colloid Interface Sci.* **169,** 168.
Bradley, R.H., Daley, R. and La Goff, F. (2002) *Carbon* **40,** 1173.
Branton, P. and Bradley, R.H. (2009) *Ext. Abstr. Carbon 2009*, Biarritz, France, June 13–19.
Branton, P. and Bradley, R.H. (2011) *Adsorption* **17,** 293.
Branton, P. and Bradley, R.H. (2010b) *Adsorpt. Sci. Technol*. **28,** 3.
Branton, P.J., Lu, A.-H. and Schüth, F. (2009) *Carbon* **47,** 1005.
Branton, P., Liu, C, Duke, M.G., Winter, D.W., Proctor, C.J. and McAdam, K.G. (2011) *Chem. Cent. J.* **5**, 15..
Burns, D.M., Dybing, E., Gray, N., Hecht, S., Anderson, C., Sanner, T., O'Connor, R., Djordjevik, M., Dresler, C., Hainaut, P., Jarvis, M., Opperhuizen, A. and Straif, K. (2008) *Tobacco Control* **17,** 132.
Coggins, C.R.E. and Gaworski, C.L. (2008) *Regul. Toxicol. Pharm*. **50,** 359.
CORESTA (1994) *CORESTA Bull. 3/4*, Recommended Method No. 40.
Dubinin, M.M. and Astakhov, V.A. (1971) *Adv. Chem. Ser.* **102,** 69.
Dubinin, M.M. and Plavnik, G.M. (1964) *Carbon* **2,** 26.
Dubinin, M.M. and Radushkevich, L.V. (1947) *Proc. Acad. Sci. USSR* **55,** 331.
Dubinin, M.M. and Serpinsky, V.V. (1981) *Carbon* **19,** 402.
Dubinin, M.M. and Timofeyev, P. (1946) *Dokl. Akad. Nauk SSSR* **54,** 701.
Everett, D.H. and Powl, J.C. (1976) *J. Chem. Soc., Faraday Trans*. **72,** 619.
Fowles, J. and Dybing, E. (2003) *Tobacco Control* **12,** 424.
Gaworski, C.L., Schramke, H., Diekmann, J., Meisgen, T.J., Tewes, F.J., Veltel, D.J., Vanscheeuwijck, P.M., Rajendran, N., Muzzio, M. and Haussmann, H.J. (2009) *Inhalation Toxicol*. **21,** 688.
Gregg, E., Hill, C., Hollywood, M., Kearney, M., McAdam, K., McLaughlin, D., Purkis, S. and Williams, M. (2004) *Beitr. Tabakforsch. Int.* **21,** 117.
Hearn, B.A., Ding, Y.S., Vaughan, C., Zhang, L., Polzin, G., Caudill, S.P., Watson, C.H. and Ashley, D.L. (2010) *Tobacco Control* **19,** 223.
ISO (2000) *ISO 3308*, "Routine Analytical Cigarette Smoking Machine — Definitions and Standard Conditions", International Organization for Standardization, Geneva, Switzerland.
Laugesen, M. and Fowles, J. (2005) *NZ Medical J*. **118,** U1402.
Laugesen, M. and Fowles, J. (2006) *Tobacco Control* **15,** 430.
Liu, C., DeGrandpré, Y., McAdam, K.G., Porter, A., Griffiths, A. and Proctor, C.J. (2011) *Food Chem. Toxicol*., published on-line, 16 March.
Marsh, H. and Rand, B. (1970) *Abstr. 3rd. Conf. Carbon and Graphite*, Society of Chemical Industry, London, p. 172.
McAdam, K.G., Gregg, E.O., Liu, C., Dittrich, D., Duke, M. and Proctor, C.J. (2011) *Food Chem. Toxicol*., **49**, 1684.
Mola, M., Hallum, M. and Branton, P. (2008) *Adsorption* **14,** 335.
Norman, A. (1999) in *Tobacco, Production Chemistry and Technology*, Davis, D.L., Nielsen, M.T., Eds, Blackwell Science, Malden, MA, U.S.A., pp. 353–387.
Polzin, G.M., Zhang, L., Hearn, B.A., Tavakoli, A.D., Vaughan, C., Ding, Y.S., Ashley, D.L. and Watson, C.H. (2008) *Tobacco Control* **17,** 10.
Rao, M.B., Jenkins, R.G. and Steele, W.A. (1985) *Ext. Abstr., 17th Biennial Carbon Conf*., Lexington, KY, U.S.A., p. 114.

Rees, V.W., Wayne, G.F., Thomas, B.F. and Connolly, G.N. (2007) *Nicotine Tob. Res*. **9,** 1197.
Reid, C.R. and Thomas, K.M. (2001) *J. Phys. Chem. B* **105,** 10 619.
Rodgman, A. and Green, C.R. (2003) *Beitr. Tabakforsch. Int.* **20,** 481.
Rutherford, S.W. and Coons, J.E. (2004) *Langmuir* **20,** 8681.
Sasaki, T., Matsumoto, A. and Yamashita, Y. (2008) *Colloids Surf. A* **325,** 166.
Stoeckli, H.F. (1974) *Helv. Chim. Acta* **57,** 7.
Stoeckli, H.F. (1997) *Carbon* **36,** 363.
Stoeckli, H.F., Kraehenbuehl, F. and Morel, D. (1983) *Carbon* **21,** 6.
Tokida, A., Atobe, I. and Maeda, K. (1985) *Agric. Biol. Chem*. **49,** 3109.
Von Blücher, H. and De Ruiter, E. (2004) *Pat. No. WO0038802.*
Von Blücher, H., Böhringer, B. and Giebelhausen, J.-M. (2006) *Pat. No. EP1918022*.